Research Article | Vol. 25, No. 13 | 26 Jun 2017 | OPTICS EXPRESS 14935

Optics EXPRESS

Monstar polarization singularities with elliptically-symmetric q-plates

BEN A. CVARCH,[1] BEHZAD KHAJAVI,[1,2] JOSHUA A. JONES,[1] BRUNO PICCIRILLO,[3] LORENZO MARRUCCI,[3] AND ENRIQUE J. GALVEZ[1,*]

[1]*Department of Physics and Astronomy, Colgate University, Hamilton, New York 13346, USA*
[2]*Department of Physics and Astronomy, Florida Atlantic University, Boca Raton, Florida 33431, USA*
[3]*Dipartimento di Fisica "Ettore Pancini," Università di Napoli Federico II, Complesso di Monte S. Angelo, 80126 Napoli, Italy*
[*]*egalvez@colgate.edu*

Abstract: Space-variant polarization patterns present in the transverse mode of optical beams highlight disclination patterns of polarization about a singularity, often a C-point. These patterns are important for understanding rotational dislocations and for characterizing complex polarization patterns. Liquid-crystal devices known as q-plates have been used to produce two of the three types of disclination patterns in optical beams: lemons and stars. Here we report the production of the third type of disclination, which is asymmetric, known as the monstar. We do so with elliptically-symmetric q-plates. We present theory and measurements, and find excellent agreement between the two.

OCIS codes: (260.6042) Singular optics; (260.5430) Polarization; (050.4865) Optical vortices; (030.4070) Modes.

References and links

1. L. Allen, M. Beijersbergen, R. Spreeuw, and J. Woerdman, "Orbital angular momentum of light and the transformation of laguerre-gaussian laser modes," Phys. Rev. A **45**, 8185–8189 (1992).
2. V. Y. Bazhenov, M. Vasnetsov, and M. Soskin, "Laser beams with screw dislocations in their wavefronts," JETP Lett. **52**, 429–432 (1991).
3. M. Dennis, K.O'Holleran, and M. Padgett, "Optical vortices and polarization singularities," Prog. Opt. **53**, 293–363 (2009).
4. G. Milione, H. Sztul, D. Nolan, and R. Alfano, "Higher-order Poincaré sphere, Stokes parameters, and the angular momentum of light," Phys. Rev. Lett. **107**, 053601 (2011).
5. E. J. Galvez, B. L. Rojec, V. Kumar, and N. K. Viswanathan, "Generation of isolated asymmetric umbilics in light's polarization," Phys. Rev. A **89**, 031801 1–4 (2014).
6. E. Nagali, F. Sciarrino, F. De Martini, L. Marrucci, B. Piccirillo, E. Karimi, and E. Santamato, "Quantum information transfer from spin to orbital angular momentum of photons," Phys. Rev. Lett. **103**, 013601 (2009).
7. G. Vallone, V. D'Ambrosio, A. Sponselli, S. Slussarenko, L. Marrucci, F. Sciarrino, and P. Villoresi, "Free-space quantum key distribution by rotation-invariant twisted photons," Phys. Rev. Lett. **113**, 060503 (2014).
8. M. V. Berry and J. H. Hannay, "Umbilic points on Gaussian random surfaces," J. Phys. A **10**, 1809–1821 (1977).
9. J. F. Nye, "Lines of circular polarization in electromagnetic wave fields," Proc. R. Soc. Lond. A **389**, 279–290 (1983).
10. J. V. Hajnal, "Singularities in the transverse fields of electromagnetic waves. ii. observation on the electric field," Proc. R. Soc. Lond. A **414**, 447–468 (1987).
11. S. Tidwell, D. Ford, and W. Kimura, "Generating radially polarized beams interferometrically," Appl. Opt. **29**, 2234–2239 (1990).
12. S. Quabis, R. Dorn, M. Eberler, O. Glöckl, and G. Leuchs, "Focusing light to a tighter spot," Opt. Commun. **179**, 1–7 (2000).
13. M. S. Soskin, V. Denisenko, and I. Freund, "Optical polarization singularities and elliptic stationary points," Opt. Lett. **28**, 1473–1477 (2003).
14. G. Volpe and D. Petrov, "Generation of cylindrical vector beams with few-mode fibers excited by Laguerre-Gaussian beams," Opt. Commun. **237**, 89–95 (2004).
15. A. Niv, G. Biener, V. Kleiner, and E. Hasman, "Rotating vectorial vortices produced by space-variant sub wavelength gratings," Opt. Lett. **30**, 2933–2935 (2005).
16. C. Maurer, A. Jesacher, S. Fürhapter, S. Bernet, and M. Ritsch-Marte, "Tailoring of arbitrary optical vector beams," New J. Phys. **9**, 78 (2007).
17. A. M. Beckley, T. G. Brown, and M. A. Alonso, "Full Poincaré beams," Opt. Express **18**, 10777–10785 (2010).

#293296 https://doi.org/10.1364/OE.25.014935
Journal © 2017 Received 20 Apr 2017; revised 13 Jun 2017; accepted 15 Jun 2017; published 20 Jun 2017

Optics EXPRESS

18. E. J. Galvez, S. Khadka, W. H. Schubert, and S. Nomoto, "Poincaré-beam patterns produced by non-separable superpositions of Laguerre-Gauss and polarization modes of light," Appl. Opt. **51**, 2925–2934 (2012).
19. F. Cardano, E. Karimi, S. Slussarenko, L. Marrucci, C. de Lisio, and E. Santamato, "Polarization pattern of vector vortex beams generated by q-plates with different topological charges," Appl. Opt. **51**, C1–C6 (2012).
20. V. Kumar and N. Viswanathan, "Topological structures in the poynting vector field: an experimental realization," Opt. Lett. **38**, 3886–3889 (2013).
21. S. Vyas, Y. Kozawa, and S. Sato, "Polarization singularities in superposition of vector beams," Opt. Express **21**, 8972–8986 (2013).
22. M. Beresna, M. Gecevicus, P. Kazansky, and T. Gertus, "Radially polarized optical vortex converter created by femtosecond laser nanostructuring of glass," Appl. Phys. Lett. **98**, 201101 (2011).
23. I. Moreno, J. Davis, D. Cottrell, and R. Donoso, "Encoding high-order cylindrically polarized light beams," Appl. Opt. **53**, 5493–5501 (2014).
24. E. Otte, C. Alpmann, and C. Denz, "Higher-order polarization singularities in tailored vector beams," J. Opt. **18**, 074012 (2016).
25. F. Cardano, E. Karimi, L. Marrucci, C. de Lisio, and E. Santamato, "Generation and dynamics of optical beams with polarization singularities," Opt. Express **21**, 8815–8820 (2013).
26. B. Piccirillo, S. Slussarenko, L. Marrucci, and E. Santamato, "The orbital angular momentum of light: genesis and evolution of the concept and of the associated photonic technology," Riv. Nuovo Cimento **36**, 501–554 (2013).
27. M. R. Dennis, "Polarization singularities in paraxial vector fields: morphology and statistics," Opt. Commun. **213**, 201–221 (2002).
28. I. Freund, "Möbius strips and twisted ribbons in intersecting Gauss Laguerre beams," Opt. Commun. **284**, 3816–3845 (2011).
29. B. Khajavi and E. Galvez, "High-order disclinations in space-variant polarization," J. Opt. **18**, 084003 (2016).
30. V. Kumar, G. M. Philip, and N. K. Viswanathan, "Formation and morphological transformation of polarization singularities: hunting the monstar," J. Opt. **15**, 044027 (2013).
31. E. Galvez and B. Khajavi, "Monstar disclinations in the polarization of singular optical beams," J. Opt. Soc. Am. A **34**, 568–575 (2017).
32. F. Flossmann, U. T. Schwarz, M. Maier, and M. R. Dennis, "Polarization singularities from unfolding an optical vortex through a birefringent crystal," Phys. Rev. Lett. **95**, 253901 (2005).
33. M. R. Dennis, "Polarization singularity anisotropy: determining monstardom," Opt. Lett. **33**, 2572–2574 (2008).
34. V. Vasil'ev and M. Soskin, "Topological and morphological transformations of developing singular paraxial vector light fields," Opt. Commun. **281**, 5527–5540 (2008).
35. S. Slussarenko, A. Murauski, T. Du, V. Chigrinov, L. Marrucci, and E. Santamato, "Tunable liquid crystal q-plates with arbitrary topological charge," Opt. Express **19**, 4085–4090 (2011).
36. B. Piccirillo, V. Kumar, L. Marrucci, and E. Santamato, "Pancharatnam-berry phase optical elements for generation and control of complex light: generalized superelliptical q-plates," Proc. SPIE **9379**, 937907 (2015).
37. G. Ruane, G. Swartzlander Jr., S. Slussarenko, L. Marrucci, and M. Dennis, "Nodal areas in coherent beams," Optica **2**, 147–150 (2015).
38. L. Marrucci, C. Manzo, and D. Paparo, "Optical spin-to-orbital angular momentum conversion in inhomogeneous anisotropic media," Phys. Rev. Lett. **96**, 163905 1–4 (2006).
39. L. Marrucci, E. Karimi, S. Slussarenko, B. Piccirillo, E. Santamato, E. Nagali, , and F. Sciarrino, "Spin-to-orbital conversion of the angular momentum of light and its classical and quantum applications," J. Opt. **13**, 064001 (2011).
40. X. Yi, X. Ling, Z. Zhang, Y. Li, X. Zhou, Y. Liu, S. Chen, H. Luo, and S. Wen, "Generation of cylindrical vector vortex beams by two cascaded metasurfaces," Opt. Express **22**, 17207–17215 (2014).
41. S. Delaney, M. M. Sánchez-López, I. Moreno, and J. A. Davis, "Arithmetic with q-plates," Appl. Opt. **56**, 596–600 (2017).
42. J. Gielis, "A generic geometric transformation that unifies a wide range of natural and abstract shapes," Am. J. Bot. **90**, 333–338 (2003).

1. Introduction

Research on complex light has brought a deeper understanding of light and features of optical beams not previously recognized, such as orbital angular momentum [1] and optical singularities [2]. Polarization singularities, and disclinations in particular, are features that contain optical information in the vectorial character of the light [3]. They have emerged as avenues to explore fundamental optical spaces [4], the study of topological disclinations [5], and their use as means to encode quantum information [6, 7]. In this article we focus on topological disclinations [8], which can be encoded in the polarization of the light [9–24].

Topological disclinations can be of three kinds: lemon, star and monstar [8]. The index of disclination I_C is the number of rotations of the polarization orientation per turn around the

Optics EXPRESS

singularity. Lemons have positive index and stars have negative index. In the far field, the center of the disclination is a point of circular polarization where the orientation is undefined, also known as a C-point [9]. Another characteristic of the disclination is the number of radial lines. These are straight lines that originate at the singularity. The polarization-ellipse orientations are radial at all points along a radial line [9]. For example, lemons with $I_C = +1/2$ and stars with $I_C = -1/2$ have one and three radial lines, respectively [8]. The symmetric patterns of lemons and stars have been studied extensively for low and high indices by numerous means: sub-wavelength structures [15,22], stress birefringence [17], superposition [16,18,20,21,23,24] and q-plates [19,25,26].

The third type of disclination is the monstar [8, 9, 27]. This disclination is asymmetric and appears when the degree of asymmetry exceeds a certain value, after which gives rise to a distinct number of radial lines than lemons or stars with the same index [28, 29]. For example, for the case of $I_C = +1/2$ the lemon has one radial line, but the monstar with the same index has 3 radial lines. Monstars have been produced only by superposition [5, 29–31]. Asymmetric polarization disclinations in random speckle fields are ubiquitous, of which 5% are monstars [27, 32–34]. Recently, monstars embedded in optical beams have been prepared with high indices [29], which include negative and zero values [31]. In this work we study the deliberate production of monstars using q-plates. These are liquid-crystal-based optical elements that have been engineered to have a spatial disclination encoded in the director of the liquid crystal molecules within a cell [35]. We implement monstar patterns by using q-plates with a disclination carrying elliptical symmetry [36, 37].

This article has been organized as follows. In Sec. 2 we present the theory describing the operation of elliptic q-plates and how we use them to create monstar patterns. Section 3 presents our experimental technique and results. Discussion and conclusions drawn are presented in Sec. 4.

2. Q-plates

Q-plates are nematic liquid-crystal cells where a disclination of order q has been encoded in the director (molecular alignment direction) of the liquid crystal molecules. Usually the director pattern in the disclination is circularly symmetric and the angular orientation ψ of the director forms a simple relation with the angular coordinate ϕ [19]. In general, this disclination pattern can be made non-circularly symmetric. Here we use q-plates that follow an elliptical symmetry [36, 37]. The method used to make q-plates is based on the rate of change of the director of the liquid crystals with the geometric angle [35], and so the angular orientation of the director is given by

$$\psi = q \tan^{-1} \left[a \tan(\phi + \gamma) \right] + \alpha, \tag{1}$$

where a is a constant that specifies the pattern ellipticity of the q-plate. More precisely, considering a standard circularly-symmetric q-plate as starting reference, a gives the spatial dilation along one direction relative to the orthogonal one. The orientation of the liquid-crystal directors forms an angle α with the lines describing the disclination pattern, and the pattern as a whole may be rotated by an angle γ.

The most common type of q-plate is the circularly-symmetric one, where $a = 1$. If we consider an unrotated q-plate ($\gamma = 0$), then if $\alpha = 0$, the liquid-crystal directors follow the lines in the disclination pattern, and so

$$\psi = q\phi. \tag{2}$$

Figures 1(a) and 1(b) show disclination patterns for $q = 1/2$ and $q = 1$, respectively. When the disclination has elliptical symmetry, the rate of change of the orientation is not linear with the angular variable, as described by Eq. (1). Figure 1(c) shows an elliptically-symmetric disclination with with $q = 1/2$ and $a = 4$.

Optics EXPRESS

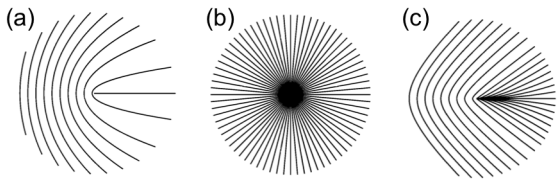

Fig. 1. Line patterns with a disclination. In (a) and (b) the patterns are circularly symmetric, with $a = 1$, but with disclination orders $q = 1/2$ and $q = 1$, respectively. In (c) the pattern is elliptically deformed with $a = 4$, and disclination order $q = 1/2$. When $\alpha = \gamma = 0$ the director orientation for q-plates follow the lines in the patterns.

The orientation angle ψ represents the fast or slow axis of a waveplate of retardation δ. The retardation can be tuned by the application of an electric field. When $\delta = \pi$, the q-plate behaves as a spatially-variable half-wave plate. If the orientation of the input polarization is $\theta_{\rm in}$, then the polarization leaving the plate will be oriented at

$$\theta = 2\psi - \theta_{\rm in}. \tag{3}$$

Thus, if $q = 1/2$, $a = 1$, $\gamma = 0$ and $\theta_{\rm in} = 0$, then the orientation of the polarization will follow $\theta = \phi$ and the light beam will be radially polarized. Similarly, if $\theta_{\rm in} = \pi/2$, then $\theta = \phi - \pi/2$ and the output will be azimuthally polarized [19].

When $\delta \neq \pi$, the q-plate behaves as a retarder having a spatially-variable optic axis and fixed retardation δ. If a circularly polarized beam in a fundamental Gaussian mode is sent to a circularly-symmetric q-plate, we obtain a symmetric disclination in the orientation of the polarization of the outgoing beam [25]. We can explain this in the following way. As a matter of notation, we express the right- and left-circularly polarized states respectively as $\hat{e}_R = 2^{-1/2}(\hat{e}_x - i\hat{e}_y)$ and $\hat{e}_L = 2^{-1/2}(\hat{e}_x + i\hat{e}_y)$, where $\hat{e}_x$ and $\hat{e}_y$ represent the linear horizontal and vertical polarization basis, respectively. In a linear basis rotated by an angle ψ, the right and left polarization are given by

$$\hat{e}_R = \frac{1}{\sqrt{2}}(\hat{e}_\psi - i\hat{e}_{\psi_\perp})e^{-i\psi} \tag{4}$$

and

$$\hat{e}_L = \frac{1}{\sqrt{2}}(\hat{e}_\psi + i\hat{e}_{\psi_\perp})e^{+i\psi}, \tag{5}$$

where $\hat{e}_\psi$ and $\hat{e}_{\psi_\perp}$ are the respective linear basis vectors rotated by angle ψ. When a circularly polarized beam is incident on a waveplate with retardation δ, the polarization of the outgoing beam is to within an overall phase given by [36]

$$\hat{U}_\delta \hat{e}_R = \cos\left(\frac{\delta}{2}\right)\hat{e}_R + i\sin\left(\frac{\delta}{2}\right)e^{-i2\psi}\hat{e}_L \tag{6}$$

$$\hat{U}_\delta \hat{e}_L = \cos\left(\frac{\delta}{2}\right)\hat{e}_L + i\sin\left(\frac{\delta}{2}\right)e^{i2\psi}\hat{e}_R \tag{7}$$

If we use a q-plate with retardation δ and orientation given by Eq. (1), then when $\delta = \pi$ (and $a = 1$), the output polarization is in the opposite circular state but with a phase that varies with 2ϕ, so that the q-plate imparts orbital angular momentum to the beam [38, 39]. When $\delta \neq \pi$ the outgoing beam has spatially-variable polarization. For a right-handed input circular wave, the relative phase between the circular output components in Eq. (6) is then

$$\Delta\varphi = \varphi_R - \varphi_L = 2\psi - \pi/2. \tag{8}$$

Optics EXPRESS

Because the orientation of the semi-major axis of the polarization is half the relative phase between the two circular polarization components, the orientation of the polarization in the pattern varies with ϕ, giving rise to a disclination. A similar result appears when the input is left-circular [25].

The disclination in the polarization is a lemon in the previous cases. It can be a star by interchanging the states of polarization with an additional half-wave plate. For a given elliptically-symmetric q-plate we found two ways to produce monstars. If $\delta = \pi/2$ and $\alpha = \gamma = 0$, and input circularly polarized, the orientation of the output polarization is given by

$$\theta = \frac{1}{2}\tan^{-1}(a\tan\phi). \tag{9}$$

The condition for radial lines, $\theta = \phi$ [5], leads to an equation in terms of $\tan\phi$, giving solutions for the angles at which we should see radial lines:

$$\tan\phi = 0, \pm\sqrt{1-\frac{2}{a}}. \tag{10}$$

For $q = 1/2$ the q-plate with $a = 1$ produces symmetric lemon patterns and only one radial line, at $\phi = 0$. When the asymmetry parameter a is increased from 1, the pattern becomes asymmetric, and for $a > 2$, two additional radial lines appear to form a monstar. For $a = 4$ the two additional radial lines appear at $\pm 35.3°$. The elliptical symmetry of this type of monstar is similar to the one obtained by non-separable modal superpositions [5].

Monstars can also be produced with the q-plate set at $\delta = \pi$ by inputting a radial beam to the q-plate. If we apply Eq. (3) with $\theta_{\text{in}} = \phi$, it leads to

$$\theta = 2\psi - \phi, \tag{11}$$

which when setting the radial-line condition $\theta = \phi$ results in the same solutions for the directions of the radial lines given by Eq. (10), with the only difference that the index of the pattern is zero. A similar monstar index of zero prepared by modal superpositions was reported recently [31].

3. Measurements

We used the apparatus shown in Fig. 2 to create and image monstar patterns. The figure shows a general schematic that was modified for several types of experiments. An optical beam from a HeNe laser was sent through a single-mode fiber. The beam emerging from a fiber collimator was sent through a polarizer and if necessary a quarter-wave plate, to set the initial state of polarization. A pair of lenses (L_1 and L_2) expanded the beam and gave it a planar wavefront. We confirmed this with a shear interferometer. The optical beam was incident on a first q-plate. The light at the plane of the q-plate was re-imaged onto a second plane, where in some cases we had a second q-plate, and in other cases two half-wave plates (H_1 and H_2 serving as circular phase shifters or linear rotators). The light in this plane was imaged onto a digital camera preceded by polarization filters. The imaging of the light in between planes was done by lenses in 4-f configuration. The size of the beam at the camera was of the order of a few millimeters. We also removed the last lens to image the beam in the far field. A set of optical elements (e.g., a quarter-wave plate and a polarizer) and neutral-density filters were used to do imaging polarimetry of the space-variant polarization pattern.

3.1. One q-plate

When the input beam with polarization set to linear-horizontal illuminated a suitably oriented symmetric q-plate with $q = 1/2$, $a = 1$ and $\delta = \pi$, it created a radial beam with polarization orientation similar to that shown in Fig. 1(b). A radial beam has index $I_C = 1$. When we used

Optics EXPRESS

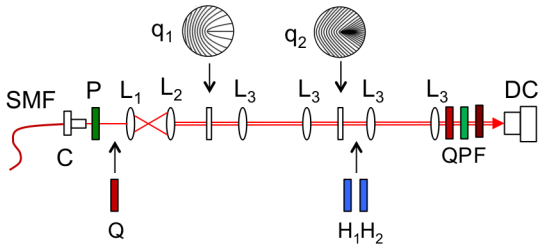

Fig. 2. Schematic of the apparatus used to perform the experiments. Optical elements include optical beam from a HeNe laser launched through a single-mode fiber (SMF) and collimator lens (C), lenses for beam expanding and imaging (L_i), q-plates (q_i), quarter (Q) and half (H) waveplates, polarizers (P), filter(s) (F) and digital camera (DC).

an elliptically-symmetric q-plate instead of a circularly-symmetric one, the index of the pattern of the beam was still 1, but the pattern was no longer radial. Figure 3(a) shows the disclination pattern that is expected from a q-plate with $a = 4$ measured in the far field. In this case the input polarization was horizontal but the pattern was rotated by 36°. Because $\alpha = 18°$, we had to adjust the orientation of the q-plate to $\gamma = -36°$ for the output to be radial-like. Figure 3(a) shows the simulation of the pattern for this situation. Note that there are purely radial lines in only four orthogonal directions. The false color in the data of Fig. 3(b) encodes the radial orientation of the polarization, with yellow encoding the radial direction. It can be seen that the agreement is very good.

By adding a pair of half-wave plates after the q-plate, as shown in Fig. 2, we were able to rotate the pattern and null the effect of α. When the input polarization was set to vertical, the circularly-symmetric q-plate produced an azimuthally-polarized beam. With the elliptically-symmetric q-plate, and compensating for α, the pattern turned into an elliptical one, with a slightly dumbbell-like shape, as shown in Fig. 3(c). The measurements shown in Fig. 3(d), taken in the near field, indeed show a linearly polarized beam with a pattern that is consistent with the expectation. The dumbbell shape is not as clear in the data. We have done other experiments with a q-plate with $a = 10$, where the data show a more pronounced dumbbell shape.

The polarization patterns discussed above are not monstars. We can make the monstar pattern

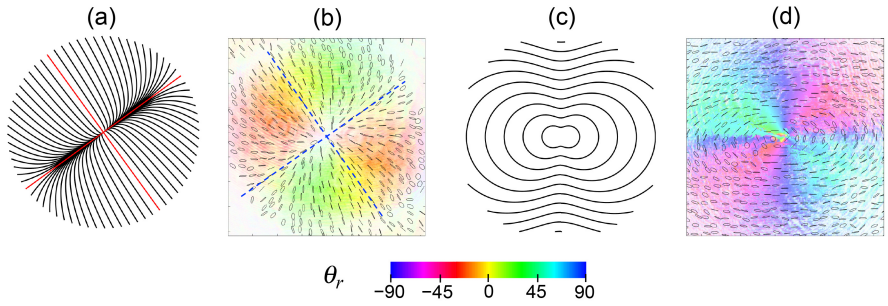

Fig. 3. Polarization of the light arising from a single elliptically-symmetric q-plate. When $\delta = \pi$ and the input polarization is linear horizontal, a q-plate with $a = 4$, and $\alpha = 18°$ produces a quasi radial pattern, modeled in (a) and measurement in the far field in (b). When the input polarization is vertical and phase-shifted to cancel the effect of the angle α, we obtained the pattern modeled in (c) and measured in (d). False color encodes the orientation of the polarization relative to the radial direction: $\theta_r = \theta - \phi$. Angles are in degrees.

Optics EXPRESS

of Fig. 1(c) with a single q-plate. To make that pattern we need to input a beam with circular polarization and tune the voltage of the q-plate for $\delta \sim \pi/2$. However, for making the pattern we needed to insert an additional phase between the circular components to obtain the orientation of Eq. (9). The pair of half-wave plates also worked to our advantage as they inserted a relative phase between the circular components allowing a nulling of α for this situation as well. Figures 4(a) and (b) show the modeled and measured patterns, respectively. Directions marking the radial orientations (in yellow) are in qualitative agreement with the expectation. See Sec. 4 for a more quantitative comparison. It can be seen that the data is consistent with having 3 radial lines. We can also see that the pattern takes the same shape as the q-plate, exhibiting an index $I_C = q = 1/2$.

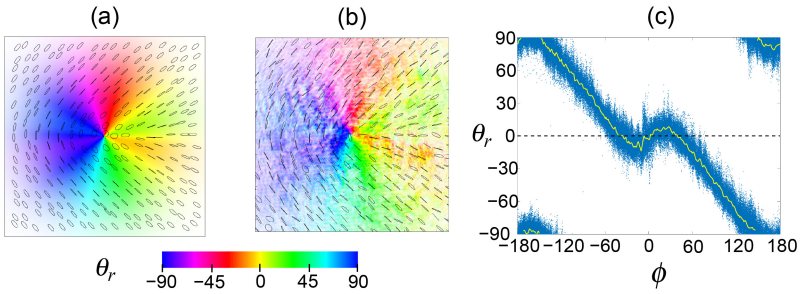

Fig. 4. Polarization of the light arising from a single elliptical q-plate with the input right circular polarization, $\delta = \pi/2$ and $a = 4$. The modeled is shown in (a) and the measured one in (b). False color encodes the orientation of the polarization relative to the radial direction θ_r. (c) is a graph of θ_r for each measured point (blue dots), with solid line representing the average value. Angles are in degrees.

The radial lines in the monstar disclination appear because the orientation relative to the radial direction,

$$\theta_r = \theta - \phi, \tag{12}$$

becomes non-monotonic in its increase or decrease along a path around the singularity [31, 33]. In Fig. 4(c) we graph the radial orientation θ_r as a function of ϕ for a central section of the image 200 × 200 pixels in size. (The image of Fig. 4(b) is 300 × 300 pixels.) There is quite a large variance in the angular orientations, as can be gathered by the thickness in the spread of the data points. The graph also includes an average of the orientation of all points at a given angular position, which is shown by the solid (yellow) line in the graph. The radial orientation of the polarization displays two non-monotonic sections, one about $\phi = 0$ and another one, not as clearly visible, about $\phi = \pm 180°$. These non-monotonic features are known to be a characteristic of monstars [31, 33]. When these features occur around $\theta_r = 0$ they gives rise to the additional radial lines seen for this case.

3.2. *Two q-plates*

The second method of making a monstar used two q-plates. As mentioned above via Eq. (11), the polarization that is input to the elliptical q-plate has to be radial. This can be accomplished by first sending uniform horizontally polarized light through a symmetric q-plate with $q = 1/2$ and $\delta = \pi$. When the second q-plate has $q = 1/2$ and $\delta = \pi$ but with $a = 4$, it transforms the polarization orientation to follow the space-variant pattern of Fig. 5(a), which has $I_C = 0$. We can understand this pattern in the following way. The incident horizontally-polarized beam has no disclination (i.e., with $I_C = 0$). It goes through a circularly-symmetric spatially-variable half-wave plate with fast axis forming an angle $\phi/2$ with the input polarization, yielding a beam

Optics EXPRESS

with a polarization orientation ϕ, or radial, with a disclination $I_C = +1$. If the second q-plate were identical to the first one, then the light would return to being horizontally polarized with $I_C = 0$, but since the second q-plate is an elliptically-symmetric one, it returns the beam to have $I_C = 0$, but with a polarization pattern distorted from being purely horizontal: carrying an asymmetric monstar disclination.

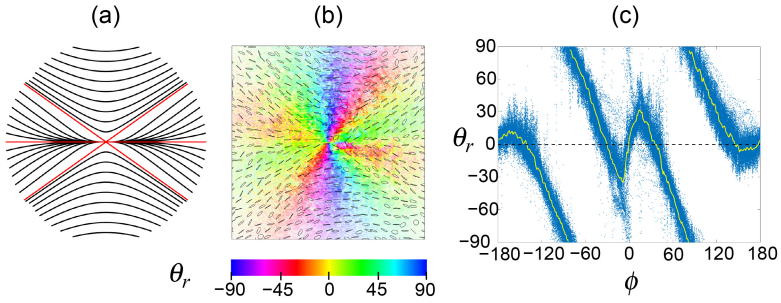

Fig. 5. Polarization results obtained when using two q-plates ($\delta = \pi$ for both), with one of them circularly-symmetric to prepare a radial beam, and a second one elliptically-symmetric to generate a monstar pattern. The final pattern is modeled in (a), with red lines showing the radial lines. (b) shows a the imaging polarimetry of the measured pattern, with false color representing the polarization orientation relative to the radial direction θ_r. (c) is a graph of θ_r for a 200 × 200 subset of points about the center (blue dots), with solid line representing the average value. Angles are in degrees.

In the experiments we adjusted the relative angle between the initial linear polarization and the first q-plate to compensate for $\alpha \neq 0$ in the second q-plate. As a result, the polarization emerging from the first q-plate had a spiral, rather than radial orientation. This light was imaged onto a second q-plate via two lenses in a 4-f arrangement. The second q-plate had either $a = 4$ or $a = 10$. Figure 5(b) shows the measured space-variant pattern obtained with the q-plate with $a = 4$. The observed polarization orientation is consistent with the modeling of Fig. 5(a). We use false color to highlight the radial-line features of the disclination (in yellow). We can clearly see six directions where the polarization is radial, matching approximately the directions of the disclination in Fig. 5(a). To obtain an accurate measure of the angles at which the radial orientations occur we plotted θ_r in Fig. 5(c), confirming the comparison from another perspective.

4. Discussion and conclusions

The data shown previously give unambiguous evidence of the general pattern of monstars. A more quantitative comparison reveals the degree to which experimental imperfections affect the measured pattern. From the graphs of Figs. 4(c) and 5(c) we obtained the angles at which the average radial orientation crossed zero (i.e., the radial lines). The case $I_C = 0$ shows 6 radial lines: 3 about $\phi = 0$ and 3 about $\phi = 180°$. In the case of $I_C = 1/2$, there are 3 radial lines about $\phi = 0$. However, in Fig. 4(c) we also see a non-monotonic section in the radial orientation about $\phi = \pm 180°$. That is, when the radial orientation is $\pm 90°$. These are orientations perpendicular to the radial direction, which also reveal a monstar-type of asymmetry [33]. These are noteworthy because they result from the same q-plate features that created radial lines at corresponding angles in the $I_C = 0$ pattern. We measured those angles as well. We further smoothed the curves of Figs. 4(c) and 5(c) to obtain more accurate values. We summarize these results in Table 1. We see a general agreement between the measurements and the expectations. In doing an investigation of the variation of the angles in the table for slight misalignments

Optics EXPRESS

Table 1. Measured angles (in degrees) of radial lines and lines perpendicular to radial (for $I_C = 1/2$) from the data of Figs. 4(c) and 5(c). The predicted values are also listed.

$I_C = 1/2$	$I_C = 0$	Predicted
$+37 \pm 5$	$+33 \pm 3$	$+35.3$
-2 ± 7	$+2 \pm 2$	0
-38 ± 4	-31 ± 3	-35.3
$-38 \pm 5 + 180$	$-33 \pm 3 + 180$	$-35.3 + 180$
$-5 \pm 7 + 180$	$+3 \pm 6 + 180$	180
$+30 \pm 8 + 180$	$+38 \pm 5 + 180$	$+35.3 + 180$

of up to 4 degrees in the orientation of the q-plate, we found values that departed from the expected positions by up to about 7 degrees. The uncertainties listed in the table are the standard deviations of these measurements. These results reveal a high sensitivity to the exact alignment of the q-plate and perhaps suggest that the phase that we use to compensate for α and γ may introduce some systematic errors.

We have also done experiments with three consecutive q-plates, with two of them elliptically symmetric. We observed that additional eliptical q-plates accentuate the asymmetry of the pattern. It has been shown previously that one can manipulate the charge of the disclination by use of consecutive q-plates [40, 41]. In the second case presented in this work, a first q-plate increased the index by 1 and the second one decreased it by 1. Should we insert a half-wave plate in between the two q-plates, we would increase the disclination to 2 [41], plus adding the corresponding asymmetry. Thus, one could use cascaded q-plates to change the asymmetry and the disclination index to obtain more complex patterns. The elliptical symmetry of the q-plates used in this work was used to study asymmetric monstar patterns that are similar to the ones obtained with first-order modal superpositions [5]. The use of q-plates with generalized superelliptical symmetry [36] may be used to study high-order disclinations, which have been shown to be present in a wide range of living systems [42]. The use of q-plates for these and other high-order patterns may offer a greater practical advantage over superposition schemes due to the more complex modal superposition that may be required to implement them.

In conclusion, monstars are structural features of polarization singularities. They reveal topological features, disclinations, that are present in many other physical systems. In this article we showed that q-plates designed with a particular deviation from circular symmetry can be used to generate all 3 types of disclinations, including monstars. We also confirmed the existence of zero-index monstars reported recently in modal superpositions [31]. When an elliptical q-plate with $\delta \sim \pi/2$ is illuminated with circular polarization, the orientation of the polarization reflects the disclination pattern of the q-plate, as shown before with symmetric q-plates [25]. It confirms that any arbitrary disclination pattern encoded onto a q-plate can be imparted in the polarization pattern of the light.

Funding

National Science Foundation (NSF) PHY1506321.

Acknowledgments

We thank S. Slussarenko for help with the fabrication of the elliptical q-plates.